Infrared emission spectra of BeH_2 and BeD_2

A. Shayesteh, K. Tereszchuk, and P. F. Bernath[a)]
Department of Chemistry, University of Waterloo, Waterloo, Ontario N2L 3G1, Canada

R. Colin
Laboratoire de Chimie Physique Moléculaire, Université Libre de Bruxelles, C.P. 160/09, 50 av. F. D. Roosevelt, 1050 Brussels, Belgium

(Received 30 September 2002; accepted 2 December 2002)

High resolution infrared emission spectra of beryllium dihydride and dideuteride have been recorded with a Fourier transform spectrometer. The molecules were generated in a discharge-furnace source, at 1500 °C and 333 mA discharge current, with beryllium metal and a mixture of helium and hydrogen or deuterium gases. The antisymmetric stretching modes (ν_3) of BeH_2 and BeD_2, as well as several hot bands involving ν_1, ν_2, and ν_3, were rotationally analyzed and spectroscopic constants were determined. The equilibrium rotational constant (B_e) of BeH_2 was found to be 4.753 66(2) cm^{-1}, and the equilibrium bond distance (R_e) of 1.326 407(3) Å was determined for BeH_2. © *2003 American Institute of Physics.* [DOI: 10.1063/1.1539850]

INTRODUCTION

BeH_2 is a famous molecule. The chemical bonding in BeH_2 is discussed in many introductory chemistry textbooks, in the context of the formation of *sp* hybrid orbitals.[1] Since BeH_2 has only six electrons, it is a favorite target molecule for quantum chemists to test their new *ab initio* methods.[2–6] However, the high toxicity of beryllium-containing compounds[7] has inhibited experimental work. According to Hinze *et al.*,[8] the insertion of ground state Be atoms into the H_2 bond has a barrier of 203.5 kJ/mol (48.6 kcal/mol), and the overall reaction

$$Be(g)+H_2(g)\rightarrow BeH_2(g)$$

has been predicted[9] to be exoergic by 157.3 kJ/mol (37.6 kcal/mol). BeH_2 was calculated[10] to be linear and to have an equilibrium bond length of 1.3324 Å, close to the recently observed value of 1.342 436 Å for the BeH free radical.[11]

In spite of this strong interest in BeH_2, the molecule remained unknown except for the detection[12] of its infrared spectrum in an argon matrix at 10 K, and in a silicon crystal as an impurity.[13] In the series of first row hydrides, LiH, BeH_2, BH_3, CH_4, NH_3, OH_2, and FH, it was the only free molecule remaining to be discovered. We recently reported in a short note the first observation of gaseous BeH_2 (Ref. 14) in a discharge-furnace emission source.

Solid BeH_2 is well-known.[15] The structure was assumed to have linear polymeric chains of Be atoms joined together by two bridging H atoms.[16] This commonly accepted ''fact'' is in error. The observed crystal structure is based on a three-dimensional arrangement of connected BeH_4 tetrahedra.[17] Heating solid BeH_2 results in decomposition to the elements,[15] not the production of gaseous molecule. The BeH_2 molecule is, however, one of the few metal dihydrides that is stable (in the thermodynamic sense) with respect to the metal vapor and molecular hydrogen. FeH_2 is the only other metal dihydride known in the gas phase,[18] except for a comment about the electronic spectrum of AlH_2 in an appendix of Herzberg's book on polyatomics.[19] We report here the observation and detailed analysis of the ν_3 antisymmetric stretching fundamental bands and several hot bands of both BeH_2 and BeD_2.

EXPERIMENTAL DETAILS

The high resolution infrared emission spectra of BeH_2 and BeD_2 were recorded with a Bruker IFS 120 HR Fourier transform spectrometer at the same time that we recorded the BeH and BeD spectra.[11] A new emission source with an electrical discharge inside a high temperature furnace was used to make the molecules. Powdered beryllium metal (about 5 g) was placed inside a zirconia boat in the center of an alumina tube (5 cm×120 cm). The central part of the tube was heated to 1500 °C by a CM Rapid Temp furnace, and the end parts were cooled by water and sealed with CaF_2 windows. A slow flow of helium (about 20 Torr) and hydrogen or deuterium (a few Torr) was passed through the cell. Two stainless steel tube electrodes were placed inside the cool ends of the tube, and a dc discharge (2.5 kV, 333 mA) was struck between them. A CaF_2 lens was used to focus the emitted light from the source into the entrance aperture of the spectrometer.

The BeH_2 spectrum was recorded in the 1800–2900 cm^{-1} spectral region at an instrumental resolution of 0.03 cm^{-1} using a CaF_2 beamsplitter. A liquid nitrogen-cooled InSb detector was used, and 200 scans were co-added. The spectral band pass was set by the detector and a 2900 cm^{-1} long-wave pass filter.

The BeD_2 spectrum was recorded (200 scans) in the spectral region of 1200–2200 cm^{-1} with the same instrumental resolution using a liquid nitrogen-cooled HgCdTe (MCT) detector. In this case the bandpass was set by the CaF_2 beamsplitter and a 2200 cm^{-1} long-wave pass filter.

a)Author to whom correspondence should be addressed; electronic mail: bernath@uwaterloo.ca

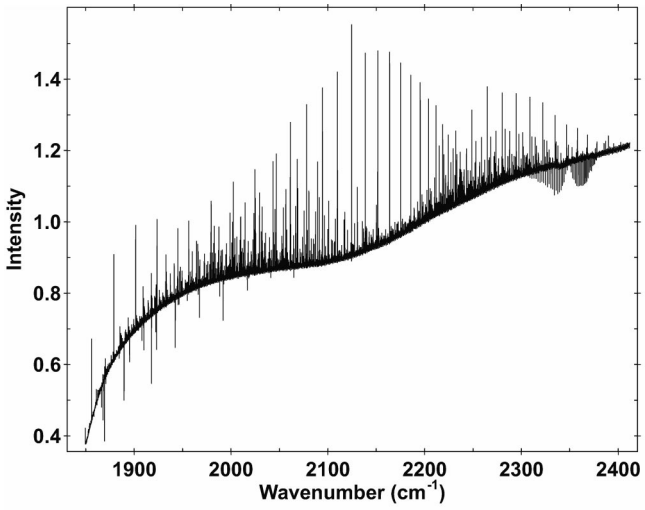

FIG. 1. An overview of the infrared emission spectrum of BeH_2 recorded with the InSb detector. All BeH lines are below 2240 cm^{-1}, and the strong emission lines above 2240 cm^{-1} are from the antisymmetric stretching (ν_3) fundamental band of BeH_2. The absorption of atmospheric CO_2 can be seen near 2350 cm^{-1}.

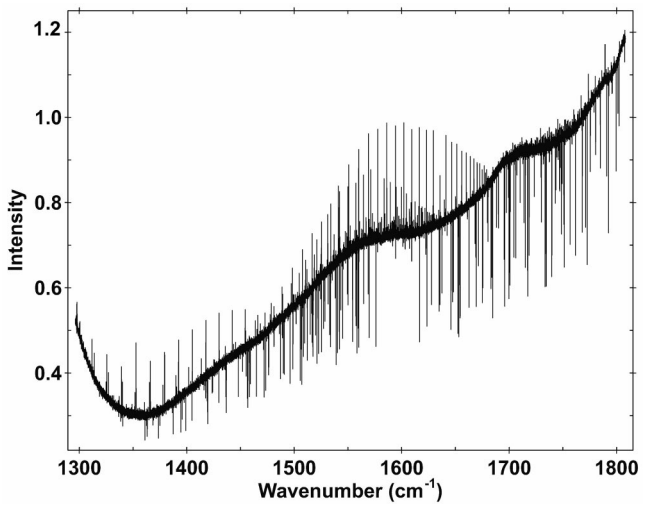

FIG. 3. An overview of the infrared emission spectrum of BeD_2 recorded with the HgCdTe detector. All BeD lines are below 1680 cm^{-1}, and the weak emission lines near 1750 cm^{-1} are from the antisymmetric stretching (ν_3) fundamental band of BeD_2. The strong absorption of atmospheric H_2O can be seen.

Atomic and molecular emission lines were present in the spectra, as well as absorption lines from atmospheric CO_2 and H_2O. The signal-to-noise ratio for the strongest BeH_2 lines was about 150.

RESULTS AND ANALYSIS

The strongest emission lines in the BeH_2 spectrum (Fig. 1) are the *R* branch lines of the BeH $v=1\rightarrow0$ band, and all BeH lines are below 2240 cm^{-1}. In addition, there are several series of lines with alternating 3:1 intensities (Fig. 2) that were assigned to BeH_2 transitions. This spectrum had channeling in the baseline that we could not eliminate in spite of our efforts. In the BeD_2 spectrum (Fig. 3), the BeD $v=1\rightarrow0$ band is the strongest series and all BeD lines are below 1680 cm^{-1}. This spectrum was unfortunately plagued by water absorption lines from the short atmospheric path between the cell and the spectrometer. There are also a few series of lines with alternating 2:1 intensities (Fig. 4) that were assigned to BeD_2.

Line positions in the spectra were determined using the WSPECTRA program, from M. Carleer (Université Libre de Bruxelles). The BeH_2 spectrum was calibrated using impurity CO emission lines, and the BeH_2 lines have an absolute accuracy of better than 0.001 cm^{-1}. The calibration of BeD_2 spectrum was based on five lines that were common with a previously calibrated BeH spectrum in the 1200–2200 cm^{-1} region. Assignment of the bands was carried out with the aid of a color Loomis–Wood program.

The strongest series of lines with intensity alternation in both BeH_2 and BeD_2 spectra were assigned to the antisymmetric stretching fundamental, 001–000, $\Sigma_u^+-\Sigma_g^+$ transi-

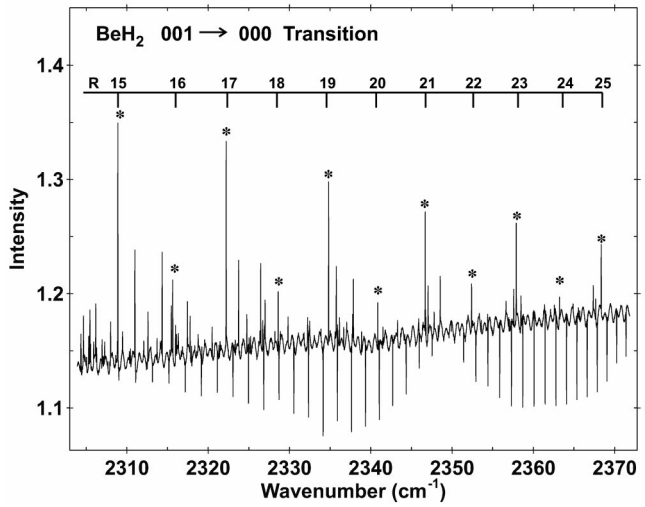

FIG. 2. An expanded view of the R branch of the 001→000 band of BeH_2 with 3:1 intensity alternation. The absorption lines are from atmospheric CO_2.

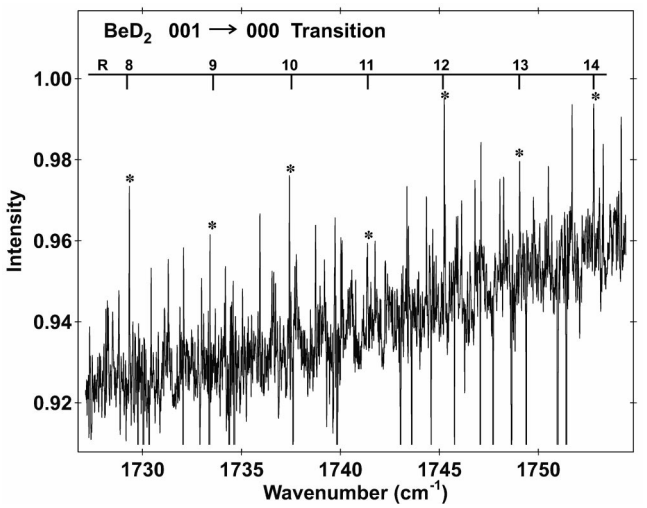

FIG. 4. An expanded view of the *R* branch of the 001→000 band of BeD_2 with 2:1 intensity alternation. The strong absorption lines are from atmospheric H_2O.

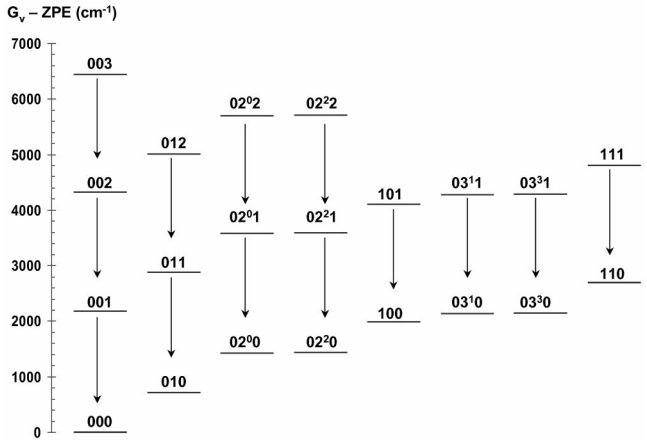

FIG. 5. An energy level diagram for BeH_2 showing the observed emission bands. The vibrational energies have been calculated with Eq. (4) using a combination of experimental and theoretical constants (see the text).

tions. The next intense series were assigned to the first bending mode hot band, 011–010, $\Pi_g-\Pi_u$ transitions. All the hot bands are shifted to the lower wave numbers because of anharmonicity. The 3:1 intensity ratio of adjacent lines in BeH_2 and the 2:1 ratio in BeD_2 arise from the *ortho–para* nuclear spin statistical weights with $(I+1)/I$ ratio.[20]

The rotational assignment of the fundamental band of BeH_2 was made based on the "missing line" at the band origin, and a small perturbation at $J'=22$, which is due to an interaction between 001 (Σ_u^+) and $03^10(\Pi_u)$ vibrational levels. In the BeD_2 fundamental band, we found the rotational assignment from a small perturbation at $J'=29$, which is due to the same interaction as in BeH_2. The absolute rotational assignments of the hot bands were not easy, because the band origins could not be predicted with the required accuracy. For BeH_2 we assigned the bands based on the $B_{v_1v_2v_3}$ values, with[20]

$$B_{v_1v_2v_3}=B_e-\alpha_1(v_1+\tfrac{1}{2})-\alpha_2(v_2+1)-\alpha_3(v_3+\tfrac{1}{2}). \quad (1)$$

We used the *ab initio* α_1 and α_2 values,[9] as well as B_{000} and α_3 from the ν_3 fundamental band, to predict the $B_{v_1v_2v_3}$ values for various vibrational levels. For each band we considered several rotational assignments, and we accepted the one nearest to the predicted $B_{v_1v_2v_3}$ value.

The following bands (Fig. 5) were assigned for BeH_2:

001–000	$\Sigma_u^+-\Sigma_g^+$,		
011–010	$\Pi_g-\Pi_u$,	002–001	$\Sigma_g^+-\Sigma_u^+$,
012–011	$\Pi_u-\Pi_g$,	003–002	$\Sigma_u^+-\Sigma_g^+$,
101–100	$\Sigma_u^+-\Sigma_g^+$,	111–110	$\Pi_g-\Pi_u$,
02^01-02^00	$\Sigma_u^+-\Sigma_g^+$,	02^21-02^20	$\Delta_u-\Delta_g$,
02^02-02^01	$\Sigma_g^+-\Sigma_u^+$,	02^22-02^21	$\Delta_g-\Delta_u$,
03^11-03^10	$\Pi_g-\Pi_u$,	03^31-03^30	$\Phi_g-\Phi_u$.

In BeD_2 we assigned five bands:

001–000	$\Sigma_u^+-\Sigma_g^+$,		
011–010	$\Pi_g-\Pi_u$,	002–001	$\Sigma_g^+-\Sigma_u^+$,
02^01-02^00	$\Sigma_u^+-\Sigma_g^+$,	02^21-02^20	$\Delta_u-\Delta_g$.

We could not find the 110–000, $\Pi_u-\Sigma_g^+$ combination band, or any other combination bands in our spectra.

The value of α_2 in BeH_2 is negative, and considerably smaller in magnitude than the α_1 and α_3 values. The 011–010 band of BeD_2 was rotationally assigned so that it yielded a reasonable α_2 value compared to α_2 in BeH_2. All the $\Pi-\Pi$ transitions showed a large *l*-type doubling, and we used the energy expression:

$$E(v_1,v_2,v_3,J)=G(v_1,v_2,v_3)+F(J), \quad (2)$$

with[20]

$$F(J)=BJ(J+1)-DJ^2(J+1)^2+HJ^3(J+1)^3 \pm \tfrac{1}{2}[qJ(J+1)+q_DJ^2(J+1)^2+q_HJ^3(J+1)^3] \quad (3)$$

in our least-squares fitting program. The observed line positions and the outputs of the least-squares fits for all the bands have been placed in Electronic Physics Auxiliary Publication Service (EPAPS).[21] The band constants in Tables I and II were determined for BeH_2 and BeD_2 using Eq. (3), in which $q=q_D=q_H=0$ for Σ states, and the plus (minus) sign refers to $e(f)$ parity. For a given J in Π states, the *e* parity lies below the *f* parity in energy, and the *l*-type doubling parameter q is negative (rather than the traditional positive value) for the 010 vibrational level.

TABLE I. Spectroscopic constants (in cm^{-1}) of BeH_2 (all uncertainties are 1σ).

Level	G_v-ZPE	B	10^4 D	10^9 H	10^2 q	10^6 q_D	10^{10} q_H
000 Σ_g^+	0.0	4.701 398 52(747)	1.049 985(168)	2.7175(100)			
001 Σ_u^+	2178.865 906(205)	4.632 187 25(689)	1.033 120(145)	2.631 73(820)			
002 Σ_g^+	4323.782 804(295)	4.564 259 00(684)	1.017 027(141)	2.571 71(770)			
003 Σ_u^+	6434.108 813(474)	4.497 254 3(109)	0.998 463(506)	2.001 2(728)			
010[a] Π_u	*a*	4.712 233 95(599)	1.090 965(120)	3.048 59(714)	−9.140 65(116)	8.1214(234)	−8.000(139)
011 Π_g	*a*+2165.882 529(162)	4.642 962 78(563)	1.074 817(110)	2.987 98(620)	−9.098 80(112)	8.0347(219)	−7.987(124)
012 Π_u	*a*+4298.243 253(256)	4.574 960 51(584)	1.059 394(114)	2.947 92(629)	−9.060 33(114)	7.9762(222)	−8.168(122)
100[a] Σ_g^+	*b*	4.644 418 1(138)	1.042 413(274)	2.7895(168)			
101 Σ_u^+	*b*+2120.153 214(256)	4.574 112 3(130)	1.026 031(247)	2.6557(143)			
110[a] Π_u	*c*	4.654 705 5(140)	1.082 079(436)	3.0902(383)	−9.021 92(274)	8.6389(850)	−13.372(749)
111 Π_g	*c*+2106.857 965(242)	4.584 407 4(132)	1.066 978(382)	3.0546(314)	−8.973 79(264)	8.5964(761)	−13.771(624)

[a]The estimated values of *a*, *b*, and *c* are 713, 1981, and 2696 cm^{-1}, respectively (see the text).

TABLE II. Spectroscopic constants (in cm^{-1}) of BeD_2 (all uncertainties are 1σ).

Level	G_v-ZPE	B	10^5 D	10^{10} H	10^2 q	10^6 q_D	10^{10} q_H
000 Σ_g^+	0.0	2.360 987 2(124)	2.620 62(262)	3.213(173)			
001 Σ_u^+	1689.678 781(334)	2.330 282 8(127)	2.589 97(295)	5.177(212)			
002 Σ_g^+	3356.735 331(589)	2.299 905 9(150)	2.516 52(380)	2.883(293)			
010[a] Π_u	a'	2.367 845 2(177)	2.693 39(400)	1.572(275)	−3.017 54(352)	1.9011(798)	−4.711(550)
011 Π_g	a'+1680.588 327(369)	2.337 135 2(180)	2.671 20(428)	5.191(320)	−3.029 90(359)	2.0133(850)	−6.211(632)

[a]The value of a' is aproximately 532 cm^{-1} (Ref. 12).

The following expression was used for the vibrational energy:

$$\begin{aligned} G(v_1,v_2,v_3) = {} & \omega_1(v_1+\tfrac{1}{2})+\omega_2(v_2+1)+\omega_3(v_3+\tfrac{1}{2}) \\ & +x_{11}(v_1+\tfrac{1}{2})^2+x_{22}(v_2+1)^2 \\ & +x_{33}(v_3+\tfrac{1}{2})^2+x_{12}(v_1+\tfrac{1}{2})(v_2+1) \\ & +x_{13}(v_1+\tfrac{1}{2})(v_3+\tfrac{1}{2})+x_{23}(v_2+1) \\ & \times(v_3+\tfrac{1}{2})+g_{22}l_2^2. \end{aligned} \quad (4)$$

In Tables I and II the vibrational energies are determined as the difference between $G(v_1,v_2,v_3)$ and the zero point energy (ZPE). We could not determine the absolute positions of all of the observed energy levels and have called the unknown values a, b, c, and a' in Tables I and II. However, some of the constants in Eq. (4) can be determined from experimental data, and the *ab initio* values[10] can be used for undetermined constants. Using a combination of experimental and theoretical constants, the numerical values of a, b, and c in Table I are roughly estimated to be 713, 1981, and 2696 cm^{-1}, respectively. The a' value in Table II is approximately 532 cm^{-1} based on a matrix isolation experiment.[12]

l-TYPE RESONANCE

Although the splitting between Δ state e/f parity levels ($l_2=\pm 2$) should be very small and negligible, for both BeH_2 and BeD_2 we observed a large splitting in all the vibrational levels with $l_2=2$ due to *l*-type resonance. The detailed theory of *l*-type resonance between Σ^+ ($l_2=0$) and Δ ($l_2=2$) states was first derived by Amat and Nielsen,[22] and was expanded later.[23–25] The Σ^+ state levels have e parity and they interact with Δ state e levels. Following Maki and Lide,[23] the Hamiltonian matrix [Eq. (5)] was used for Σ^+ (e) and Δ (e) levels in fitting the 02^01-02^00, 02^21-02^20, 02^02-02^01, and 02^22-02^21 bands of BeH_2.

$$\boldsymbol{H}=\begin{pmatrix} E_\Sigma^0 & \sqrt{2}W_{20} \\ \sqrt{2}W_{20} & E_\Delta^0 \end{pmatrix}. \quad (5)$$

The diagonal matrix elements are the ordinary energy expressions for Σ^+ and Δ states:

$$\begin{aligned} E^0 = {} & G(v_1,v_2,v_3)+BJ(J+1) \\ & -DJ^2(J+1)^2+HJ^3(J+1)^3, \end{aligned} \quad (6)$$

while the off-diagonal term has the following form:

$$\begin{aligned} W_{20} = {} & \frac{1}{\sqrt{2}}[q+q_DJ(J+1)+q_HJ^2(J+1)^2] \\ & \times(J^2(J+1)^2-2J(J+1))^{1/2}. \end{aligned} \quad (7)$$

No interaction affects the Δ state f levels and we used Eq. (6) for the f parity.

The constants of Table III were determined for BeH_2 with an *l*-resonance fit of the corresponding bands. The value of d in Table III is roughly estimated to be 1420 cm^{-1}, and the difference between Σ^+ and Δ states origins is equal to $4g_{22}$ [Eq. (4)]. The Δ states vibrational energies in Table III are higher than those of corresponding Σ^+ states, which is consistent with a positive g_{22} predicted by *ab initio* calculations.[10] We found fitting errors (smaller than 0.1 cm^{-1}) for the line positions of Δ–Δ transitions, but the Σ^+–Σ^+ transitions fitted very well within the experimental uncertainty. This additional perturbation is caused by the 050 and 051 vibrational levels that are close to 021 and 022 levels, respectively. There are three states with $l_2=1$, 3, and 5 (Π, Φ, and H) for the 050 and 051 levels, and we assume that the Φ states (05^30 and 05^31) are perturbing the Δ states

TABLE III. Spectroscopic constants (in cm^{-1}) of BeH_2 for levels involving *l*-type resonance (all uncertainties are 1σ).

Level	l	G_v-ZPE	B	10^4 D	10^9 H	10^2 q	10^6 q_D	10^{10} q_H
020[a]	0	d	4.723 696 6(172)	1.140 252(405)	3.7571(278)			
						−9.179 95(132)	8.2333(254)	−7.573(157)
	2	d+8.200 88(553)	4.722 444 51(995)	1.134 571(234)	3.6242(160)			
021	0	d+2152.984 78(146)	4.653 428 5(784)	1.109 73(251)	2.988(225)			
						−9.119 10(429)	7.852(104)	−6.123(603)
	2	d+2161.090 45(772)	4.653 488 5(490)	1.124 32(219)	3.806(219)			
022	0	d+4272.893 08(249)	4.584 354(154)	1.079 17(646)	2.306(586)			
						−9.056 07(864)	7.410(345)	−4.79(295)
	2	d+4280.918 1(115)	4.585 760 4(932)	1.114 75(363)	4.024(341)			

[a]The estimated value of d is 1420 cm^{-1} (see text).

TABLE IV. Spectroscopic constants (in cm^{-1}) of BeD_2 for levels involving *l*-type resonance (all uncertainties are 1σ).

Level	l	G_v-ZPE	B	10^5 D	10^{10} H	10^2 q	10^6 q_D
020[a]	0	d'	2.375 102 0(514)	2.892 1(130)	10.312(990)		
						−2.971 45(121)	1.0799(125)
	2	$d'+0.598\ 33(987)$	2.374 545 2(315)	2.820 90(788)	5.367(577)		
021	0	$d'+1671.503\ 13(170)$	2.344 428 3(550)	2.873 0(141)	13.52(111)		
						−2.978 27(120)	1.0478(124)
	2	$d'+1672.161\ 1(104)$	2.343 858 9(314)	2.820 00(810)	12.788(628)		

[a]The estimated value of d' is 1064 cm^{-1} (obtained as 2 times ν_2 from the matrix value reported in Ref. 12).

(02^21 and 02^22). We added the 02^00 and 02^20 states combination differences in our fit (with 0.0015 cm^{-1} weight), and deweighted the 02^21-02^20 and 02^22-02^21 lines to 0.1 cm^{-1}. As a result, the 020 constants (Table III) were determined accurately, but the 021 and 022 constants have only moderate precision and accuracy. A more complete analysis of the various resonances was not attempted.

The 02^01-02^00 and 02^21-02^20 bands of BeD_2 were fitted using the same *l*-resonance matrix elements, and the corresponding constants were determined (Table IV). In this case, we did not observe any perturbation in the 021 vibrational level. However, the number of observed lines was smaller and we had to fix $q_H=0$ for the 020 and 021 levels of BeD_2.

The 03^11-03^10, $\Pi_g-\Pi_u$, and 03^31-03^30, $\Phi_g-\Phi_u$ bands of BeH_2 showed *l*-type resonance between Π and Φ states in both *e* and *f* parity levels. According to the positive sign of g_{22}, the Φ states have higher energy than the Π states. There is also a large *l*-type doubling in the Π states, which splits the *e* and *f* parity levels. The splitting increases with J [Eq. (3)], and the *f* parity levels of Π and Φ states cross at $J\approx13$. Because of this crossing, we could not determine any reasonable constants for the 030 and 031 vibrational levels.

DISCUSSION

The intensity alternation in both BeH_2 and BeD_2 lines is consistent with a linear structure with $D_{\infty h}$ symmetry. The equilibrium structure of BeH_2 and some constants of BeD_2 can be determined from the band constants of Tables I–IV. The experimental constants of BeH_2 are compared with the *ab initio* values[10] in Table V. We found bands involving all three vibrational modes of BeH_2 and α_1, α_2, α_3, and B_e were determined (Table V) using B_{000}, B_{100}, B_{010}, and B_{001} values and Eq. (1), but for BeD_2 we could determine only α_2 and α_3. The equilibrium rotational constant (B_e) of BeH_2 was found to be 4.753 66(2) cm^{-1}, in good agreement with the theoretical value of Martin and Lee.[10] The equilibrium Be–H distance (R_e) was calculated to be 1.326 407(3) Å using the B_e value of Table V, while the *ab initio* value[10] of R_e is 1.3324 Å. The 001–000 band origin (ν_3) of BeH_2 is 2178.8659(2) cm^{-1}, close to the theoretical value[10] of 2167.2 cm^{-1} and to the matrix isolation value[12] of 2159 cm^{-1}. Our ν_3 value of 1689.6788(3) cm^{-1} for BeD_2 is also in reasonable agreement with the matrix isolation value[12] of 1674 cm^{-1}.

Using the origins of 001–000, 101–100, 011–010, and 002–001 bands with Eq. (4), some anharmonicity constants (x_{13}, x_{23}, x_{33} of BeH_2 and x_{23}, x_{33} of BeD_2) were obtained. The equilibrium frequency of the antisymmetric stretching mode ω_3 was calculated for BeH_2 using ν_3, x_{13}, x_{23}, and x_{33}. Our ω_3 value of 2255.155(1) cm^{-1} is close to the *ab initio* value of 2249.4 cm^{-1}. The *l*-type doubling constant q for the Π states is related to B_e, ω_2, and ω_3 by[19,23]

$$q=-\frac{B_e^2}{\omega_2}\left(1+\frac{4\omega_2^2}{\omega_3^2-\omega_2^2}\right)(v_2+1). \tag{8}$$

Using B_e, ω_3, and q_{010} values, the equilibrium bending mode frequency (ω_2) of BeH_2 was calculated to be 716.5 cm^{-1}, very close to the theoretical value of 717.7 cm^{-1}. We

TABLE V. Equilibrium constants of BeH_2 and BeD_2 (in cm^{-1}).

Constant	BeH_2 (this work)	BeH_2 (Martin and Lee[a])	BeD_2 (this work)
R_e/Å	1.326 407(3)	1.332 4	⋯
R_0/Å	1.333 758(1)	1.339 7	1.331 361(4)
B_e	4.753 66(2)	4.711 17	⋯
$D_e\times10^4$	1.021 2(5)	1.007 9	⋯
$H_e\times10^9$	2.39(3)	2.5	⋯
α_1	0.056 98(2)	0.055 76	⋯
α_2	−0.010 84(1)	−0.011 83	−0.006 86(2)
α_3	0.069 21(1)	0.069 96	0.030 70(2)
q_{010}	−0.091 41(1)	(−0.0896)[b]	−0.030 18(4)
ν_1 (σ_g)	⋯	1979.6	⋯
ν_2 (π_u)	⋯	716.8	⋯
ν_3 (σ_u)	2178.865 9(2)[c]	2167.2	1689.678 8(3)[d]
ω_1	⋯	2037.3	⋯
ω_2	716.5[e]	717.7	⋯
ω_3	2255.155(1)	2249.4	⋯
x_{11}	⋯	−14.29	⋯
x_{12}	⋯	1.80	⋯
x_{13}	−58.712 7(3)	−61.84	⋯
x_{22}	⋯	(+0.52)[b]	⋯
x_{23}	−12.983 4(3)	−11.68	−9.090 5(5)
x_{33}	−16.974 5(3)	−19.78	−11.311 1(4)
g_{22}	2.050(1)	2.46	0.150(2)

[a]Reference 10.

[b]The value of −0.002 71 cm^{-1} for q_{010} is in error in Ref. 10. A more recent value using the same approach but a slightly different basis set is −0.0896 cm^{-1}, in excellent agreement with our data. In addition, the sign of x_{22} is erroneous in Ref. 10, the value should be +0.52 cm^{-1} (Ref. 27).

[c]The matrix isolation values (Ref. 12) of ν_2 and ν_3 are 698 and 2159 cm^{-1}, respectively.

[d]The matrix isolation values (Ref. 12) of ν_2 and ν_3 are 532 and 1674 cm^{-1}, respectively.

[e]Calculated from the q_{010} value and Eq. (8).

also determined g_{22} for both molecules from the *l*-type resonance constants in Tables III and IV. Our g_{22} value of 2.050(1) cm^{-1} for BeH_2 is in reasonable agreement with the *ab initio* value of 2.46 cm^{-1}.

CONCLUSION

The high resolution infrared emission spectra of BeH_2 and BeD_2 at 1500 °C were recorded with a Fourier transform spectrometer. The antisymmetric stretching modes ν_3 of both molecules, as well as ten hot bands of BeH_2 and four hot bands of BeD_2 were rotationally analyzed. From the equilibrium rotational constant (B_e) of BeH_2, the equilibrium Be–H distance (R_e) was determined to be 1.326 407(3) Å. Our work represents the first complete rotational analysis (B_e and three α_i's) and equilibrium structure for a metal dihydride. The discharge-furnace emission source and the technique of high resolution infrared emission spectroscopy[26] are powerful tools for generating and studying high temperature metal hydrides.

ACKNOWLEDGMENTS

This work was supported by the Natural Sciences and Engineering Research Council (NSERC) of Canada and by the Fonds National de la Recherche Scientifique (FNRS) of Belgium.

[1] For example, S. R. Radel and M. H. Navidi, *Chemistry* (West Publishing, St. Paul, 1990), p. 390.
[2] P. G. Szalay and R. J. Bartlett, J. Chem. Phys. **103**, 3600 (1995).
[3] U. S. Mahapatra, B. Datta, and D. Mukherjee, J. Chem. Phys. **110**, 6171 (1999).
[4] D. A. Mazziotti, Phys. Rev. A **60**, 4396 (1999).
[5] R. Baer and D. Neuhauser, J. Chem. Phys. **112**, 1679 (2000).
[6] Y. G. Khait and M. R. Hoffmann, J. Chem. Phys. **108**, 8317 (1998).
[7] S. Budavari, M. J. O'Neil, A. Smith, and P. E. Heckelman, *The Merck Index*, 11th ed. (Merck, Rahway 1989), pp. 181–183.
[8] J. Hinze, O. Friedrich, and A. Sundermann, Mol. Phys. **96**, 711 (1999).
[9] J. M. L. Martin, Chem. Phys. Lett. **273**, 98 (1997).
[10] J. M. L. Martin and T. J. Lee, Chem. Phys. Lett. **200**, 502 (1992).
[11] A. Shayesteh, K. Tereszchuk, P. F. Bernath, and R. Colin, J. Chem. Phys. **118**, 1158 (2003). (in press).
[12] T. J. Tague, Jr. and L. Andrews, J. Am. Chem. Soc. **115**, 12111 (1993).
[13] R. Mori, N. Fukata, M. Suezawa, and A. Kasuya, Physica B **302-303**, 206 (2001).
[14] P. F. Bernath, A. Shayesteh, K. Tereszchuk, and R. Colin, Science **297**, 1323 (2002).
[15] N. N. Greenwood and A. Earnshaw, *Chemistry of the Elements* (Pergamon, Oxford, 1984), p. 125.
[16] G. J. Brendel, E. M. Marlett, and L. M. Niebylski, Inorg. Chem. **17**, 3589 (1978).
[17] G. S. Smith, Q. C. Johnson, D. K. Smith, D. E. Cox, R. L. Snyder, R.-S. Zhou, and A. Zalkin, Solid State Commun. **67**, 491 (1988).
[18] H. Körsgen, W. Urban, and J. Brown, J. Chem. Phys. **110**, 3861 (1999).
[19] G. Herzberg, *Electronic Spectra of Polyatomic Molecules* (Van Nostrand Reinhold, New York, 1966), p. 583.
[20] P. F. Bernath, *Spectra of Atoms and Molecules* (Oxford University Press, New York, 1995).
[21] See EPAPS Document No. JCPSA6-118-016308 for the observed line positions and the outputs of the least-squares fits for all the bands. A direct link to this document may be found in the online article's HTML reference section. The document may also be reached via the EPAPS homepage (http://www.aip.org/pubservs/epaps.html) or from ftp.aip.org in the directory /epaps/. See the EPAPS homepage for more information.
[22] G. Amat and H. H. Nielsen, J. Mol. Spectrosc. **2**, 163 (1958).
[23] A. G. Maki, Jr. and D. R. Lide, Jr., J. Chem. Phys. **47**, 3206 (1967).
[24] D. Papoušek and M. R. Aliev, *Molecular Vibrational–Rotational Spectra* (Elsevier, Amsterdam, 1982).
[25] J. K. G. Watson, Can. J. Phys. **79**, 521 (2001).
[26] P. F. Bernath, Annu. Rep. Prog. Chem., Sect. C: Phys. Chem. **96**, 177 (2000).
[27] J. M. L. Martin and T. J. Lee (private communication).